duced evidence to suggest that, in birds, distinct allelic forms of *Lps* influence survival during Gram-negative infection. It is possible that mutations of human *Tlr4* also affect susceptibility to Gram-negative infection, or its clinical outcome.


**References and Notes**

1. R. W. Pinner *et al.*, *J. Am. Med. Assoc.* **275**, 189 (1996).
2. A. D. O'Brien *et al.*, *J. Immunol.* **124**, 20 (1980).
3. D. L. Rosenstreich, A. C. Weinblatt, A. D. O'Brien, *CRC Crit. Rev. Immunol.* **3**, 263 (1982).
4. B. M. Sultzer, *Nature* **219**, 1253 (1968).
5. D. L. Rosenstreich, M. L. Glode, S. E. Mergenhagen, *J. Infect. Dis.* **136**, S239 (1977).
6. R. N. Apte, O. Ascher, D. H. Pluznik, *J. Immunol.* **119**, 1898 (1977).
7. D. L. Rosenstreich, S. N. Vogel, A. R. Jacques, L. M. Wahl, J. J. Oppenheim, *ibid.* **121**, 1664 (1978).
8. S. M. Michalek, R. N. Moore, J. R. McGhee, D. L. Rosenstreich, S. E. Mergenhagen, *J. Infect. Dis.* **141**, 55 (1980).
9. S. N. Vogel, *Tumor Necrosis Factors: The Molecules and Their Emerging Role in Medicine*, B. Beutler, Ed. (Raven, New York, 1992), p. 485.
10. A. Coutinho and T. Meo, *Immunogenetics* **7**, 17 (1978).
11. A. Coutinho, L. Forni, F. Melchers, T. Watanabe, *Eur. J. Immunol.* **7**, 325 (1977).
12. S. N. Vogel, C. T. Hansen, D. L. Rosenstreich, *J. Immunol.* **122**, 619 (1979).
13. P. S. Tobias, K. Soldau, R. J. Ulevitch, *J. Biol. Chem.* **264**, 10867 (1989).
14. R. R. Schumann *et al.*, *Science* **249**, 1429 (1990).
15. S. D. Wright, R. A. Ramos, P. S. Tobias, R. J. Ulevitch, J. C. Mathison, *ibid.*, p. 1431.
16. A. Haziot *et al.*, *Immunity.* **4**, 407 (1996).
17. J. Han, J.-D. Lee, P. S. Tobias, R. J. Ulevitch, *J. Biol. Chem.* **268**, 25009 (1993).
18. J. Han, J.-D. Lee, L. Bibbs, R. J. Ulevitch, *Science* **265**, 808 (1994).
19. T. D. Geppert, C. E. Whitehurst, P. Thompson, B. Beutler, *Mol. Med.* **1**, 93 (1994).
20. J. M. Kyriakis *et al.*, *Nature* **369**, 156 (1994).
21. I. Sanchez *et al.*, *ibid.* **372**, 794 (1994).
22. B. Beutler *et al.*, *ibid.* **316**, 552 (1985).
23. B. Beutler, I. W. Milsark, A. C. Cerami, *Science* **229**, 869 (1985).
24. J. Watson, R. Riblet, B. A. Taylor, *J. Immunol.* **118**, 2088 (1977).
25. J. Watson, K. Kelly, M. Largen, B. A. Taylor, *ibid.* **120**, 422 (1978).
26. A. Poltorak *et al.*, *Blood Cells Mol. Dis.* **24**, 340 (1998).
27. BLAST searches were performed against the nonredundant (NR) GenBank database, the TIGR database of ESTs, and the dbEST database of ESTs. Searches against NR and TIGR databases were performed at both the nucleotide (blastn) and amino acid (blastx) levels. dbEST searches were carried out at the nucleotide level only.
28. Obtained from Oak Ridge National Laboratory via the World Wide Web (compbio.ornl.gov/tools/index.shtml).
29. A. Poltorak *et al.*, data not shown.
30. D. B. Kuhns, P. D. Long, J. I. Gallin, *J. Immunol.* **158**, 3959 (1997).
31. Supplementary Web material for Fig. 2 is available at www.sciencemag.org/feature/data/985613.shl.
32. To monitor the efficiency of reverse transcription and PCR, we used primers specific for the transferrin receptor (TFR) as a positive control when attempting to detect the low-abundance Tlr4 mRNA in macrophage or fetal RNA samples by RT-PCR.
33. R. Medzhitov, P. Preston-Hurlburt, C. A. Janeway Jr., *Nature* **388**, 394 (1997).
34. RAW 264.7 cells, obtained from the American Type Culture Collection, are immortalized LPS-responsive cells, frequently used in studies of LPS signal transduction and TNF gene regulation. RAW 264.7 cells, like primary macrophages, become refractory to LPS for a variable interval of time after a primary stimulus with LPS.
35. J. Mathison, E. Wolfson, S. Steinemann, P. Tobias, R. Ulevitch, *J. Clin. Invest.* **92**, 2053 (1993).
36. R.-B. Yang *et al.*, *Nature* **395**, 284 (1998).
37. B. Lemaitre, E. Nicolas, L. Michaut, J. M. Reichhart, J. A. Hoffmann, *Cell* **86**, 973 (1996).
38. E. Eldon *et al.*, *Development* **120**, 885 (1994).
39. C. Chiang and P. A. Beachy, *Mech. Dev.* **47**, 225 (1994).
40. M. J. Williams, A. Rodriguez, D. A. Kimbrell, E. D. Eldon, *EMBO J.* **16**, 6120 (1997).
41. J. X. Hu *et al.*, *Genome Res.* **7**, 693 (1997).


42. We acknowledge the assistance of J. Turner, A. Powelka, R. Jain, R. Clisch, and C. Brady, all summer undergraduate research fellows who worked with us to identify the *Lps*$^d$ mutation. We are also grateful to the Beutler Family Charitable Trust for providing funds for the purchase of an ABI model 373 sequencer.

30 September 1998; accepted 3 November 1998


# Exploiting the Basis of Proline Recognition by SH3 and WW Domains: Design of N-Substituted Inhibitors


**Jack T. Nguyen, Christoph W. Turck, Fred E. Cohen, Ronald N. Zuckermann, Wendell A. Lim***



Src homology 3 (SH3) and WW protein interaction domains bind specific proline-rich sequences. However, instead of recognizing critical prolines on the basis of side chain shape or rigidity, these domains broadly accepted amide N-substituted residues. Proline is apparently specifically selected in vivo, despite low complementarity, because it is the only endogenous N-substituted amino acid. This discriminatory mechanism explains how these domains achieve specific but low-affinity recognition, a property that is necessary for transient signaling interactions. The mechanism can be exploited: screening a series of ligands in which key prolines were replaced by nonnatural N-substituted residues yielded a ligand that selectively bound the Grb2 SH3 domain with 100 times greater affinity.


Protein-protein interaction domains, such as Src homology 3 (SH3) and WW domains, participate in diverse signaling pathways and are important targets in drug design (*1*, *2*). These domains specifically recognize unique proline-rich peptide motifs but bind them with low affinities ($K_d$ = 1 to 200 μM) compared with other peptide recognition proteins such as antibodies and receptors ($K_d$ = nanomolar to picomolar concentrations). SH3 domains recognize sequences bearing the core element, PXXP (P = proline, X = any amino acid), flanked by other domain-specific residues (*3*). Identification of compounds that potently interrupt these interactions has proven difficult: extensive screening of natural and nonnatural combinatorial libraries has not yielded compounds that bind as well as or better than PXXP peptides (*4*, *5*). Here we show that the essential ligand feature recognized by both SH3 and WW domains is an irregular backbone substitution pattern: N-substituted residues placed at key positions along an otherwise normal $C^{\alpha}$-substituted peptide scaffold. Prolines are required at these sites, not on the basis of side chain


J. T. Nguyen, F. E. Cohen, W. A. Lim, Department of Cellular and Molecular Pharmacology, Department of Biochemistry and Biophysics, and Graduate Group in Biophysics, University of California, San Francisco, CA 94143, USA. C. W. Turck, Howard Hughes Medical Institute, University of California, San Francisco, CA 94143, USA. R. N. Zuckermann, Chiron Corporation, Emeryville, CA 94608, USA.

*To whom correspondence should be addressed E-mail: wlim@itsa.ucsf.edu


**Table 1.** Reduction in binding affinity (*21*) caused by alanine (A) or sarcosine (A*) substitutions within proline-rich ligands of Sem5 SH3 domain and Yap WW domain (*22*). "Required" prolines are underlined.

| Site | Peptide | $K_d^{mutant}/K_d^{wild\ type}$ | |
|---|---|---|---|
| | SH3 ligands | X = A | A* |
| Wild type | PPPVPPR | — | — |
| $P_{-3}$ | XPPVPPR | 1 | 2 |
| $P_{-2}$ | PXPVPPR | >50 | 3 |
| $P_{-1}$ | PPXVPPR | 2 | 2 |
| $P_0$ | PPPXPPR | 6 | >50 |
| $P_{-1}$ | PPPVXPR | >50 | 3 |
| $P_{-2}$ | PPPVPXR | 2 | 2 |
| | WW ligands | X = A | A* |
| Wild type | GTPPPPYTVG | — | — |
| $P_{-3}$ | GTXPPPYTVG | 1 | 7 |
| $P_{-2}$ | GTPXPPYTVG | 2 | >100 |
| $P_{-1}$ | GTPPXPYTVG | >100 | 6 |
| $P_0$ | GTPPPXYTVG | 2 | 4 |

shape but simply because they are the only naturally available N-substituted residue. This unusual recognition code has been used to guide design of SH3 inhibitors with improved affinity and selectivity.

We used a chemical minimization scheme to identify essential ligand recognition elements for two domains, the COOH-terminal SH3 domain from the *Caenorhabditis elegans* adapter protein Sem5, and the WW domain from the human signaling protein Yap. The Sem5 SH3 domain recognizes the core PXXP sequence, flanked by a specific arginine residue (*1*). WW domains recognize the consensus motif PPXY (Y = tyrosine) (*2*). We scanned through the proline-rich core of each ligand and made the following substitutions:

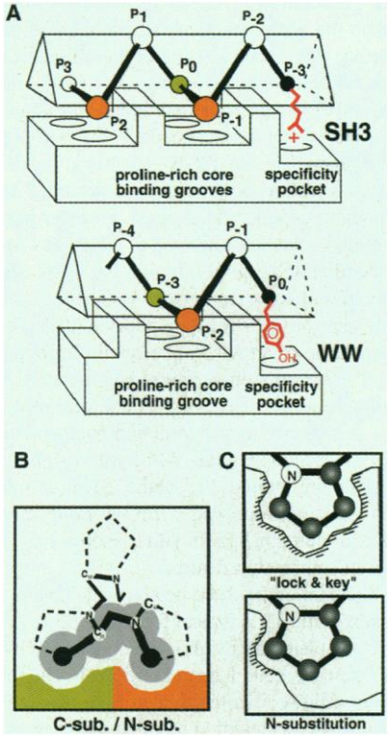


**Fig. 1.** Backbone substitution requirements for SH3 and WW domain recognition. (**A**) Structural mapping of alanine and sarcosine scanning results (Table 1). Peptide/domain complex interfaces (*8*, *9*) shown schematically. Ligands adopt a PPII conformation, depicted schematically as a triangular prism. Residue positions (spheres) are color-coded by class: white—does not require either $C^{\alpha}$- or N-substitution (alanine and sarcosine tolerant); green—requires $C^{\alpha}$-substitution (alanine tolerant, sarcosine intolerant); orange—requires N-substitution (sarcosine tolerant, alanine intolerant). (**B**) Minimally sufficient recognition unit for SH3 and WW domain binding grooves. Schematic view of a single binding groove cross-section, looking down the PPII helical axis (viewed from left side of Fig. 1A). Minimally required atoms defined in this study, a sequential pair of $C^{\alpha}$- and N-substituted residues, are solid black. The van der Waals binding surface that these atoms present is shaded. (**C**) Distinct mechanisms of proline recognition. Proline can be recognized by a lock and key mechanism, utilizing the full chemical potential of the side chain. In contrast, SH3 and WW domains recognized key prolines based on N-substitution. This mechanism utilizes relatively little of the binding potential of ligand or protein (hatched surface) but is still highly discriminatory for proline among natural amino acids.

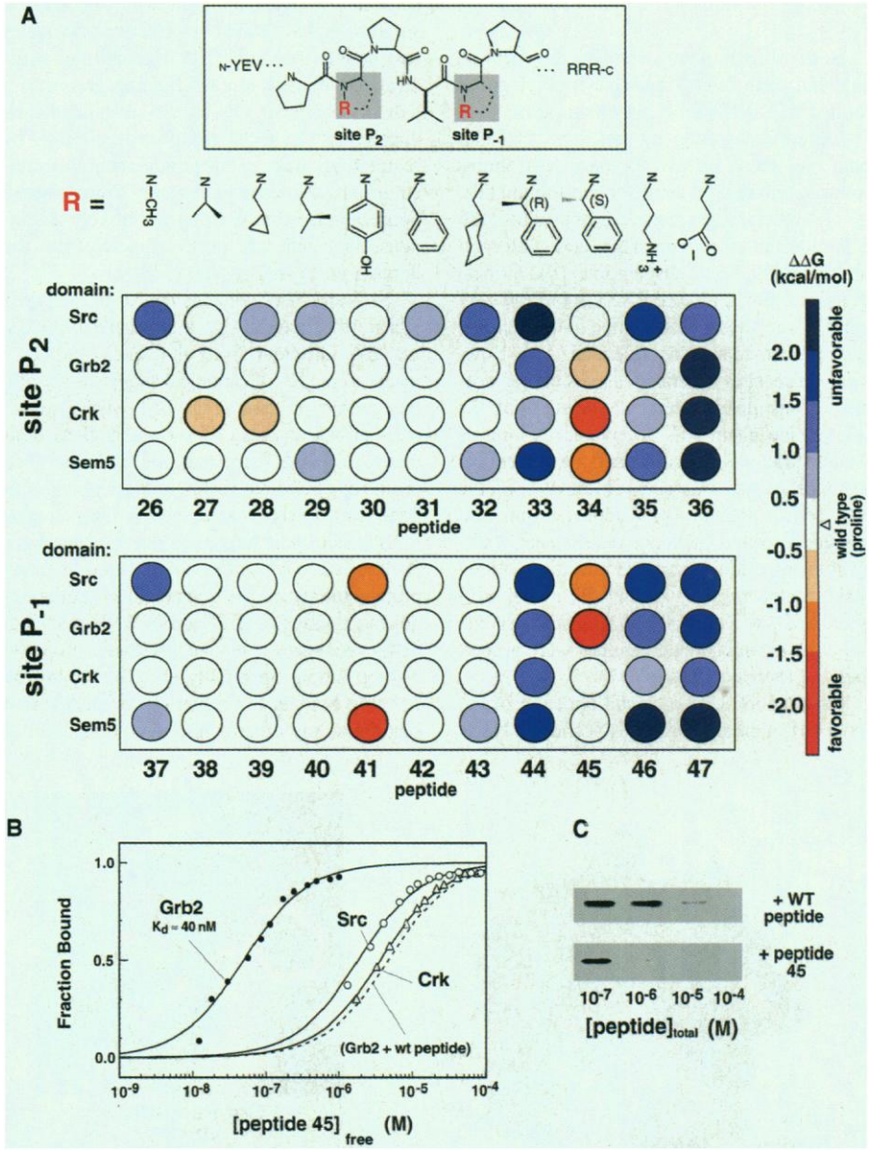


**Fig. 2.** Replacing required ligand prolines with peptoids can increase affinity and selectivity for SH3 domains. (**A**) Effects of peptoid substitutions at proline-requiring sites of SH3 ligand (*23*). Wild-type background is YEVPPPVPPRRR (*24*). Required proline sites ($P_2$ and $P_{-1}$) are shown shaded in the chemical structure. Binding was measured to the Sem5 COOH-terminal SH3 domain, the mouse Crk $NH_2$-terminal SH3 domain, the human Grb2 $NH_2$-terminal SH3 domain, and the mouse Src SH3 domain (*21*). Changes in free energy of binding upon mutation ($\Delta\Delta G$) relative to proline are color coded (orange—favorable; blue—unfavorable). Dissociation constants for the wild-type 12-mer peptide are as follows: Sem5, $K_d$ = 48 μM; Crk, $K_d$ = 6 μM; Grb2, $K_d$ = 5 μM; Src, $K_d$ = 25 μM. (**B**) Peptide 45 selectively binds Grb2 SH3 with $10^2$-fold improved affinity. Binding curve of peptide 45 [*N*-(*S*)-phenylethyl peptoid at $P_{-1}$] to Grb2 $NH_2$-terminal SH3 domain (filled circles), Src SH3 domain (white circles), and Crk SH3 domain (triangles), as measured by fluorescence perturbation. Data were fit (solid lines) as described (*21*). Data for the Sem5 SH3 domain are not shown, as this domain binds with 50-fold lower affinity than the other domains tested. For reference, isotherm of wild-type peptide binding to Grb2 is shown by a dashed line (overlaps with Crk binding curve). (**C**) Inhibition of Grb2 SH3 binding by peptide 45. Binding of biotinylated Grb2 SH3 domain to Sos peptide/GST fusion protein in the presence of peptide 45 or wild-type peptide (*25*). The $K_i$ of inhibitor is estimated to be 1/10th of the observed $IC_{50}$.

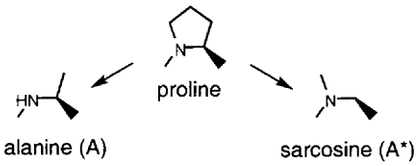


Both substitutions destroy the proline ring, but each leaves a single methyl group bonded to a different main chain atom.

Proline recognition by the Sem5 SH3 domain and the Yap WW domain was almost exclusively based on amide N-substitution (Table 1)—other unique properties of proline, such as its unusual side chain shape and conformational rigidity, were dispensable (*6*). Critical prolines of the SH3 core PXXP motif (sites $P_2$ and $P_{-1}$) are sites where alanine or other amino acid replacements are not tolerated (*1, 4*). However, these sites tolerated sarcosine replacement. Thus nearly complete deletion of the proline side chain was acceptable as long as N-substitution was maintained. An identical tolerance pattern was seen at site $P_{-2}$ of the WW domain ligand. The scanning results also revealed a second backbone requirement: a $C^{\alpha}$-substituted residue must precede the required N-substituted residue. At Site $P_0$ in the SH3 ligand and site $P_{-3}$ in the WW ligand, alanine and other $C^{\alpha}$-substituted residues were acceptable, but sarcosine was not (*7*).

Examination of the crystal structure of the Sem5 SH3 domain complex (*8*) and the NMR (nuclear magnetic resonance) structure of the Yap WW domain complex (*9*) reveals the basis for these requirements. In both complexes, the ligand binds in a polyproline II (PPII) helical conformation, a left-handed helix with three residues per turn. Turns on one face of the helix pack into a series of grooves on the domain surface (Fig. 1A). Each groove accommodates two peptide residues. The minimal and sufficient requirement at each binding groove is a pair of sequential $C^{\alpha}$- and N-substituted residues (*10*). The $C^{\alpha}$/N-substituted pair may be required because, in this arrangement, substituent groups are separated by only a single backbone carbon atom, forming a relatively continuous ridge that can pack efficiently into the domain grooves (Fig. 1B) (*11*).

SH3 and WW domains appear to read their signature sequences by a mechanism fundamentally different from the "lock and key" mechanism (*12*) of canonical sequence-specific recognition proteins (Fig. 1C). Such interactions utilize an array of surface pockets optimized to fit the shape and size of anchor side chains displayed along the ligand peptide backbone (*13*). In such cases, even small perturbations in side chain properties can be deleterious. Proline is recognized in this fashion at many protein interfaces. In contrast, the proline-requiring pockets of SH3 and WW domains actually recognize a unique backbone property: N-substitution. Specificity is achieved, not by favoring binding to proline but by disfavoring binding to any other natural amino acid, all of which lack N-substitution.

This backbone discrimination mechanism reveals a strategy for inhibitor design: maintain the required hybrid $C^{\alpha}$- and N-substituted scaffold, but vary side chain identity along this scaffold to optimize complementarity. We tested this strategy by synthesizing a series of SH3 ligands in which each of the two "required" PXXP prolines was replaced by a diverse set of 11 nonnatural N-substituted glycine, or "peptoid," residues (Fig. 2A). Such groups could exploit the untapped chemical potential of this interface. We tested binding of these ligands to four SH3 domains—Sem5, Crk, Grb2, and Src—all of which share a preference for ligands with the consensus sequence PXXPXR (*14*). More than half the 22 N-substituted ligands bound as well as or better than natural proline-containing peptides. In contrast, no other natural amino acids are tolerated at these sites (*4*).

Peptide 45 (Fig. 2B) bound the Grb2 SH3 domain with an affinity ($K_d$ = 40 nM) > 100 times that of the wild-type peptide (*15*). This substitution of an *N*-(*S*)-phenylethyl group at site $P_{-1}$ results in a favorable increase in binding energy of $\Delta\Delta G = -2.8$ kcal/mol, a 40% increase in total interaction energy. Peptide 41, which has an *N*-(4-hydroxy)phenyl substitution, bound the Sem5 SH3 domain with 25-fold improved affinity. Four other specific domain-ligand pairs showed 5- to 10-fold improved affinity.

Recognition of these peptoid side chains is stereospecific, as is typical for interactions with high complementarity. For example, the Grb2 SH3 domain bound peptide 45 with $10^3$-fold greater affinity than the related *R*-stereoisomer (peptide 44). In addition, peptide 45 acted as a potent competitive inhibitor (Fig. 2C), blocking binding of the Grb2 SH3 domain to a Sos peptide fusion protein with an $IC_{50}$ about 1/50th that of the wild-type proline peptide.

The peptoid ligands have improved domain selectivity, overcoming a second major problem posed by SH3 domains as drug targets—members of the family are highly cross-reactive (*16*). This enlarged range of N-substituted residues can be used to exploit subtle differences between individual SH3 domains. For example, peptide 45 binds potently to Grb2 but shows only modest to negligible improvement in binding to the other domains, resulting in about $10^2$-fold selectivity for Grb2 (Fig. 2B).

We crystallized and solved the structures of three SH3-peptoid ligand complexes (*17*). These structures (Fig. 3) confirmed that the peptoid side chains bound at the proline-requiring sites and suggest how peptoids increase affinity and domain discrimination. The peptoid side chains insert into these sites more deeply than proline, packing slightly differently. Thus specific side chains can make better fitting and more extensive contacts with the domain, including contacts with regions on the SH3 sur-

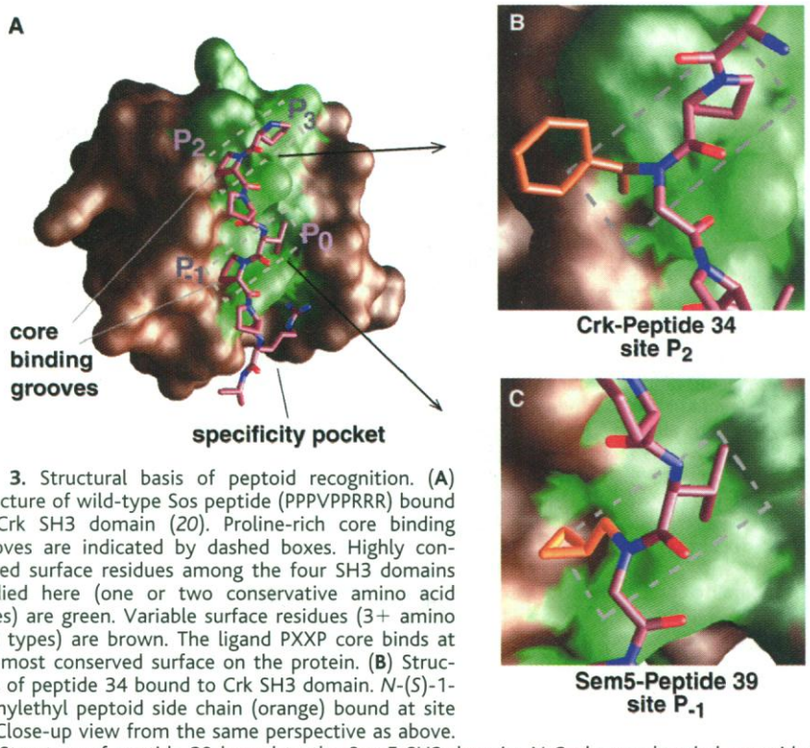


**Fig. 3.** Structural basis of peptoid recognition. (**A**) Structure of wild-type Sos peptide (PPPVPPRRR) bound to Crk SH3 domain (*20*). Proline-rich core binding grooves are indicated by dashed boxes. Highly conserved surface residues among the four SH3 domains studied here (one or two conservative amino acid types) are green. Variable surface residues (3+ amino acid types) are brown. The ligand PXXP core binds at the most conserved surface on the protein. (**B**) Structure of peptide 34 bound to Crk SH3 domain. *N*-(*S*)-1-Phenylethyl peptoid side chain (orange) bound at site $P_2$. Close-up view from the same perspective as above. (**C**) Structure of peptide 39 bound to the Sem5 SH3 domain. *N*-Cyclopropylmethyl peptoid side chain (orange) bound at site $P_{-1}$. Close-up view from the same perspective as above.

face that show higher sequence or structural variation. The chemistry of peptoid synthesis allows for exploration of greater side chain diversity than examined here and could yield optimized ligands for other SH3 domains.

The recognition strategy of SH3 and WW domains allows for high specificity binding that need not be of high affinity. In vivo, binding to proline peptides is highly selective, despite suboptimal shape complementarity, because there are no other natural sequences that can satisfy the minimal ligand backbone requirements. The resultant weak but specific interactions are ideal for intracellular signaling domains. These modules must recognize ligands with high enough selectivity to maintain proper information flow but with low enough affinity to allow for sensitive and dynamic modulation in response to changing signals. In contrast the high-affinity and high-specificity interactions that result from typical lock and key recognition are ill-suited for such a function. The ability to recognize proline in this way may explain why proline-rich motifs are so commonly used in regulatory interactions.

### References and Notes


1. G. B. Cohen, R. Ren, D. Baltimore, *Cell* **80**, 237 (1995); T. Pawson and J. D. Scott, *Science* **278**, 2075 (1997); T. E. Smithgall, *J. Pharmacol. Toxicol. Methods* **34**, 125 (1995); J. Kuriyan and D. Cowburn, *Annu. Rev. Biophys. Biomol. Struct.* **26**, 259 (1997).
2. M. Sudol, *Prog. Biophys. Mol. Biol.* **65**, 113 (1996).
3. Nearly all SH3 ligands have a PXXP motif. A notable exception is the intramolecular SH3 ligand found in Src family kinases, which in some cases has only one proline [W. Xu, S. C., Harrison, M. J. Eck, *Nature* **385**, 595 (1997); F. Sicheri, I. Moarefi, J. Kuriyan, *ibid.*, p. 595]. However, these are extremely low affinity ligands, which are not observed to bind in an intermolecular context.
4. Z. Weng *et al.*, *Mol. Cell. Biol.* **14**, 4509 (1994); A. B. Sparks *et al.*, *J. Biol. Chem.* **269**, 23853 (1994); R. J. Rickles *et al.*, *EMBO J.* **13**, 5598 (1994); R. J. Rickles *et al.*, *Proc. Natl. Acad. Sci. U S.A.* **92**, 10909 (1995); M. T. Pisabarro and L. Serrano, *Biochemistry* **35**, 10634 (1996); A. B. Sparks *et al.*, *Proc. Natl. Acad. Sci. U.S.A.* **93**, 1540 (1996); D. Grabs *et al.*, *J. Biol. Chem.* **272**, 13419 (1997).
5. T. N. Schumacher *et al.*, *Science* **271**, 1854 (1996); S. Feng *et al.*, *Chem. Biol.* **3**, 661 (1996); J. P. Morken *et al.*, *J. Am. Chem. Soc.* **120**, 30 (1998).
6. Proline has several distinct properties that could be used for recognition, including its unusually shaped pyrrolidine side chain and the conformational constraints that result from its cyclic structure. However, our data do not support a dominant energetic role for proline's conformational constraints. Breakage of the proline ring always incurs a detectable energetic cost in binding and may explain the preference for a high density of ligand prolines. However, from substitutions at apical sites, which make no contact with the domain, we estimate that the conformational cost of breaking the proline ring by either alanine or sarcosine replacement is 0.4 to 0.9 kcal/mol (affinity of one-half to one-fifth of proline). This is far smaller than the ≥2.5 kcal/mol (affinity of ≤1/100th of proline) cost of removing required $C^{\alpha}$- or N-substituted groups. Thus the conformational constraints are not a critical element in how these domains recognize key prolines. The unique ability of proline to adopt the cis peptide bond conformation also does not appear to play a role in SH3 or WW recognition because bound ligands adopt an all-trans peptide bond conformation.
7. Site $P_0$ of the SH3 ligand is included in this set because it can tolerate valine (wild-type peptide), proline, and alanine but not sarcosine (*23*). Site $P_3$ in the Sem5 SH3 ligand does not conform to this pattern of required backbone substitution, perhaps because it is at the very $NH_2$-terminus of the ligand. This site does not appear to have a dominant role in recognition and can tolerate even glycine substitutions (J.T.N., unpublished data).
8. W. A. Lim, F. M. Richards, R. O. Fox, *Nature* **372**, 375 (1994).
9. M. J. Macias *et al.*, *ibid.* **382**, 646 (1996).
10. Minimally, methyl substitution at the appropriate position appears to be required at both of these groove binding sites, because glycine, which lacks any side chain, is not tolerated (J.T.N., unpublished data). The minimal requirements defined here are within the context of a peptide scaffold. Other sequence-independent interactions may also be necessary for binding.
11. Canonical SH3 binding sequences contain two pairs of XP dipeptides (*18*). The only way to achieve the required $C^{\alpha}$-/N-substituted structure with natural amino acids is with an XP dipeptide. SH3 domains bind proline-rich peptides in two possible $NH_2$- to COOH-terminal orientations (*8*, *18*). When binding orientation is switched, the sites along the SH3 surface that require proline are switched. As shown in Fig. 1B, when binding orientation is reversed, maintenance of groove packing interactions would necessitate a reversal of sites requiring an N-substituted site (*8*). It is because the $C^{\alpha}$-/N-substituted unit is twofold rotationally symmetric that it can pack into SH3 grooves in either orientation.
12. We use the term lock and key to mean recognition of two molecules with high complementarity of shape. Complementary structures may be preformed or induced.
13. J. Janin and C. Chothia, *J. Biol. Chem.* **265**, 16027 (1990); R. L. Stanfield and I. A. Wilson, *Curr. Opin. Struct. Biol.* **5**, 103 (1995); D. R. Davies and G. H. Cohen, *Proc. Natl. Acad. Sci. U.S.A.* **93**, 7 (1996); C. Chothia and E. Y. Jones, *Annu. Rev. Biochem.* **66**, 823 (1997); J. A. Wells, *Proc. Natl. Acad. Sci. U.S.A.* **93**, 1 (1996).
14. The COOH-terminal Sem5 SH3 domain was purified as described (*8*). The $NH_2$-terminal Grb2 SH3 domain (residues 1 to 63) and the $NH_2$-terminal SH3 domain from Crk (residues 134 to191) were cloned by the polymerase chain reaction from the appropriate cDNA library. The proteins were expressed as fusions to glutathione *S*-transferase (GST) with a COOH-terminal $His_6$ tag. Proteins were purified over a glutathione column, released by thrombin cleavage, and further purified over a nickel column. The Src SH3 domain (residues 87 to 142) was cloned into a pET19b expression vector and purified over a nickel column.
15. The Hck SH3 domain has an affinity of $K_d$ = 250 nM for the intact human immunodeficiency virus Nef protein [C. H. Lee *et al.*, *EMBO J.* **14**, 5006 (1995); C. H. Lee *et al.*, *Cell* **85**, 931 (1996)]. However, in this case the PXXP motif is presented within the context of the intact, folded Nef protein structure, and extensive additional surface contacts, away from the proline-rich core, contribute to binding energy. The highest-affinity natural ligand for the Grb2 $NH_2$-terminal SH3 domain is the wild-type peptide from Sos ($K_d \approx 5$ μM) (*19*).
16. A. R. Viguera *et al.*, *Biochemistry* **33**, 10925 (1994).
17. We solved the crystal structures of the following complexes: peptide 34 bound to the Crk SH3 domain [29% PEG 4000, 0.2 M ammonium acetate (pH 6.0)]; peptide 38 bound to the Sem5 SH3 domain [in 28% PEG 4000, 0.2 M LiOAc (pH 7.5)]; and peptide 39 bound to the Sem5 SH3 domain [in 50% saturated ammonium phosphate (pH 8.0)]. These ligands bind these domains with improved affinities of 8-, 2-, and 1.1-fold, respectively. We were unable to obtain crystals of our highest-affinity ligand, peptide 45, bound to the Grb2 SH3 domain. For the Sem5 complex structures, peptoid substitutions were remade in the 9-mer background, PPPVXPRRR, required for crystal formation. Sem5 complex data were collected on a Rigaku R-AXIS IV detector (rotating anode). Crk data were collected on a Mar detector at the Stanford Synchrotron Radiation Laboratory. Data were processed with the programs Denzo and Scalepack [Z. Otwinoski and W. Minor, *Methods Enzymol.* **276**, 307 (1997)]. Molecular replacement solutions were obtained by using the program AMORE [CCP4: A Suite of Programs for Protein Crystallography (SERC Daresbury Laboratory, Warrington WA4 4AD, UK, 1979)] with either the Sem5 SH3 domain (*8*) or the Crk SH3 domain (*20*) as search models (without ligand). Structures were refined and rebuilt with the programs X-PLOR [A. T. Brunger, X-PLOR (Yale Univ. Press, New Haven, CT, 1996)] and O [T. A. Jones, J.-Y. Zou, S. W. Cowan, M. Kjelgaard, *Acta Crystallogr.* **A47**, 110 (1991)]. After several rounds of refinement, electron density for the ligand was visible. Crystallographic statistics for peptide 38/Sem5: space group $P2_1$, cell $a$ = 33.2, $b$ = 59.9, $c$ = 33.6, β =102°, α = γ = 90°, resolution 2.2 Å, completeness 99.6%, $R_{merge}$= 9.3%, $R_{factor}$ = 20.6%, $R_{free}$ = 27.9%, root mean square deviation (rmsd) bond lengths = 0.005 Å, rmsd bond angles = 1.221°. Crystallographic statistics for peptide 39/Sem5: space group $P2_1$, cell $a$ = 27.0, $b$ = 68.5, $c$ = 35.0, β = 93.9°, α = γ = 90°, resolution 2.5 Å, completeness 98.0%, $R_{merge}$= 9.0%, $R_{factor}$ = 22.6% , $R_{free}$ = 31.2%, rmsd bond lengths = 0.006 Å, rmsd bond angles = 1.124°. Crystallographic statistics for peptide 34/Crk: space group $P4_3$ , cell $a = b$ = 36.8, $c$ = 52.6, α = β = γ = 90°, resolution 2.5 Å, completeness 92.0%, $R_{merge}$= 6.9%, $R_{factor}$ = 25.0%, $R_{free}$ = 34.9%, rmsd bond lengths = 0.006 Å, rmsd bond angles = 1.142°.
18. S. Feng *et al.*, *Science* **266**, 1241 (1994).
19. S. Feng *et al.*, *Proc. Natl. Acad. Sci. U.S.A.* **92**, 12408 (1995); B. S. Knudsen *et al.*, *EMBO J.* **14**, 2191 (1995).
20. X. Wu *et al.*, *Structure* **3**, 215 (1995).
21. Dissociation constants ($K_d$) were measured by fluorescence perturbation and fit by nonlinear least-squares analysis with the program Sigmaplot or Profit [W. A. Lim, R. O. Fox, F. M. Richards, *Prot. Sci.* **3**, 1261 (1994)]. Total protein concentration, $P$, was fixed at 0.05 to 1 μM for each binding experiment, yielding conditions for most ligands in which $K_d \gg P$. For high-affinity ligands ($K_d$ < 0.5 μM), where $K_d \approx P$, data were fit to the following equation:

$$F_b = \frac{K_d + P + L \pm \sqrt{(K_d + P + L)^2 - 4 \times P \times L}}{2 \times P}$$

where $F_b$ = fraction bound and $L$ is total peptide ligand concentration. Data are the averages of two or three measurements. Errors for all measurements were between 5% and 15%.
22. These represent ligands of minimal length containing a required nonproline anchor residue (R for the Sem-5 SH3 domain, Y for the YAP WW domain) at one terminus. The Sem5 SH3 domain requires the binding motif XPXXPXR, and removal of the R results in a decrease in affinity of about 100-fold (W.A.L., unpublished data). Removal of the Y in the WW ligand also results in loss of detectable binding (*9*). Thus these nonproline anchor residues lock the ligand into only one possible binding register and orientation, making compensatory binding arrangements unlikely. Dissociation constants for the wild-type peptides ($K_d^{wild\text{-}type}$) were as follows: Sem5 SH3 domain, $K_d^{wild\text{-}type}$ = 190 μM; YAP WW domain, $K_d^{wild\text{-}type}$ = 40 μM. Peptides were synthesized on an Applied Biosystems model 431A synthesizer. Site nomenclature (sites $P_{-3}$ to $P_3$) for the SH3 ligands has been described (*8*). The site nomenclature for the WW ligand places the critical tyrosine at site $P_0$, with the residues preceding it in sequence numbered $P_{-3}$ to $P_{-1}$.
23. Full binding measurements on all peptides and peptoids are provided in supplementary material at www.sciencemag.org/feature/data/983858.shl.
24. Peptoid substitutions were synthesized in the 12-mer background, YEVPPPVPPRRR, which has a higher affinity than the 7-mer used in Table 1. This peptide from mSos is the highest-affinity natural ligand for both the Sem5 COOH-terminal SH3 domain and the Grb2 $NH_2$-terminal SH3 domain. The COOH-terminal peptide portion was synthesized on an Applied Biosystems model 431A synthesizer. Coupling of the peptoid residue was performed by the submonomer method [R. J. Simon *et al.*, *Proc. Natl. Acad. Sci. U.S.A.* **89**, 9367 (1992); G. M. Figliozzi *et al.*, *Methods Enzymol.* **267**, 437 (1996)] with the following modifications: the peptide $NH_2$-terminus was acylated by reaction with equal volumes of 1 M bromoacetic acid in dichloromethane and 1 M diisocarbodiimide in dimethylformamide (twice for 30 min); nu-

cleophilic displacement was effected with 2 M amine in dimethyl sulfoxide at 35°C for 2 hours. The subsequent Fmoc amino acid (10 equivalents) was coupled by using 10 equivalents of the coupling reagent PyBrop (NovaBiochem) and 18 equivalents of diisopropyl ethyl amine (three times for 2 hours). The remaining portion was synthesized by standard Fmoc chemistry. Peptoids were cleaved, purified by reversed-phase high-performance liquid chromatography, and verified by electrospray mass spectrometry. After lyophilization, peptoids were resuspended in water and the concentration was determined by tyrosine absorbance and by amino acid analysis.

25. Competitive inhibition of SH3 binding by peptoids was assayed by mixing the indicated concentration of inhibitor peptide with a Grb2 SH3 domain (~50 nM), expressed as a fusion to a protein that is endogenously biotinylated in *Escherichia coli* (PINPOINT vector, Promega, Madison, WI) in STE [50 mM tris-HCl (pH 8.0), 150 mM NaCl, 0.5 mM EDTA ], in a total volume of 1.5 ml for 30 min. Glutathione agarose beads (15 μl) that had been bound with ~250 nmol of a GST fusion to a tandem repeat of the Sos derived peptide $(PPPVPPRR)_2$ were added to the above mixture and incubated at 4°C for 1 hour. The agarose beads were washed with 3 × 1 ml of STE and boiled in 30 μl of SDS–polyacrylamide gel electrophoresis (SDS-PAGE) buffer, and the eluate was subjected to SDS-PAGE. The amount of biotinylated SH3 fusion retained on the beads was measured by blotting these gels onto nitrocellulose, blocking in TBST [100 mM tris-HCl (pH 8.0), 150 mM NaCl, 0.1% Tween 20) with 1% milk, probing with streptavidin–horseradish peroxidase conjugate, and developing with Pierce chemiluminescent SuperSubstrate. Under these reaction conditions, the $K_i$ is calculated to be approximately 1/10th of the observed $IC_{50}$. The observed $IC_{50}$ for peptide 45, $\sim 5 \times 10^{-7}$ M, is therefore close to the lower limit of detection for this assay, given the concentration of biotinylated SH3 used in the assay ($5 \times 10^{-8}$ M).

26. Supported by grants from the National Institutes of Health (W.A.L., F.E.C.) and awards to W.A.L from the Howard Hughes Medical Institute Research Resources Program, the Burroughs Wellcome Fund, the Searle Scholars Program, and the Packard Foundation. We are grateful to H. Yoshihara, K. Thorn, S. Ng, H. Aldaz, T. Lim, E. Ruttenberg, and E. Beausoleil for assistance, and to H. Bourne, J. Weissman, B. Honig, M. Van Gilst, D. Julius, B. Darimont, K. Earle, and members of the Lim Laboratory for helpful discussions. We thank M. Sudol for coordinates of the YAP WW domain complex structure and S. Almo and N. Mahoney for coordinates of the Profilin-$Pro_{10}$ complex structure. W.A.L. thanks F. Richards and R. Fox for their support while starting this line of investigation. J.T.N. is a National Science Foundation Predoctoral Fellow. Coordinates for the SH3/inhibitor complexes have been deposited in the Protein Data Bank (Sem5-peptide 39, ID code 3Sem; Sem5-peptide 38, ID code 2Sem; Crk-peptide 34, ID code 1b07).

15 July 1998; accepted 2 November 1998

# Defective T Cell Differentiation in the Absence of *Jnk1*

**Chen Dong,* Derek D. Yang,*† Mark Wysk, Alan J. Whitmarsh, Roger J. Davis, Richard A. Flavell‡**

The c-Jun $NH_2$-terminal kinase (JNK) signaling pathway has been implicated in the immune response that is mediated by the activation and differentiation of CD4 helper T ($T_H$) cells into $T_H1$ and $T_H2$ effector cells. JNK activity observed in wild-type activated $T_H$ cells was severely reduced in $T_H$ cells from *Jnk1*$^{-/-}$ mice. The *Jnk1*$^{-/-}$ T cells hyperproliferated, exhibited decreased activation-induced cell death, and preferentially differentiated to $T_H2$ cells. The enhanced production of $T_H2$ cytokines by *Jnk1*$^{-/-}$ cells was associated with increased nuclear accumulation of the transcription factor NFATc. Thus, the JNK1 signaling pathway plays a key role in T cell receptor–initiated $T_H$ cell proliferation, apoptosis, and differentiation.

When activated by antigen-presenting cells (APCs), $T_H$ cells undergo clonal proliferation and produce interleukin 2 (IL-2). The activated $T_H$ cells may then become $T_H1$ or $T_H2$ effector cells (*1*), which mediate inflammatory or humoral responses, respectively. The polarization of $T_H$ cell differentiation is, at least in part, determined by the cytokine environment (*1*). IL-12, produced by activated APCs, induces $T_H1$ development of naïve $T_H$ cells. IL-4, made by T cells, is required for $T_H2$ differentiation. Thus, early production of IL-4 or IL-12 determines $T_H$ cell lineage commitment and the type of immune response that occurs. Although most attention has focused on the effect of polarizing cytokines on $T_H$ cell differentiation, signals from the T cell receptor (TCR)–CD3 complex and from the costimulatory factor CD28 may also affect cytokine production by mechanisms not yet understood (*2*).

JNK, also known as stress-activated protein kinase, phosphorylates the transcription factor c-Jun and increases AP-1 transcription activity (*3, 4*). Other substrates include JunD, ATF2, ATFa, Elk-1, Sap-1, and NFAT4 (*3, 4*). Signals from both the TCR-CD3 complex and CD28 are required for JNK and AP-1 activation in T cells, and these signals may be integrated in such a way as to mediate T cell activation and the induction of IL-2 transcription (*5*). Although JNK is implicated in IL-2 gene transcription, JNK may also act to stabilize IL-2 mRNA (*6*). AP-1 has also been reported to be important for the regulation of $T_H1$ and $T_H2$ cytokine genes (*7, 8*).

To understand the role or roles of JNK in $T_H$ cell activation and differentiation, we generated *Jnk1*-deficient mice through homologous recombination in embryonic stem cells (*9*) (Fig. 1A). Targeted disruption of the *Jnk1* gene resulted in a null allele, as confirmed by mRNA (*10*) and protein expression analysis of embryonic fibroblast (Fig. 1B) and T cell (*11*) extracts. *Jnk1*-deficient mice were fertile and of normal size. Lymphocyte development appeared normal, with typical ratios of T cells to B cells, CD4 to CD8, and naïve to memory T cells in the periphery (*10*). The absence of apparent developmental defects of *Jnk1*$^{-/-}$ lymphocytes might be the result of redundancy, because *Jnk1* and *Jnk2* are coexpressed in lymphoid tissues (*4*). Therefore, we tested whether JNK1 and JNK2 are activated similarly during the course of $T_H$ cell activation.

Purified CD4 T cells from wild-type or knockout mice were stimulated by antibodies to CD3 (anti-CD3) with or without anti-CD28 (*12, 13*), and JNK activity was measured using c-Jun as the substrate. During the first 48 hours, induced JNK activity was greatly reduced in the *Jnk1*$^{-/-}$ $T_H$ cells; moreover, anti-CD28 could not enhance kinase activity (Fig. 1C). Essentially no JNK activity was detected in *Jnk1*$^{-/-}$ $T_H$ cells stimulated for only 5 min, despite the same JNK2 protein expression (*11*). Thus, JNK1 appeared to account for most of the JNK activity in newly activated T cells. After 60 hours of stimulation, JNK activity in the *Jnk1*$^{-/-}$ cells was similar to that in wild-type cells, and in each case this activity was presumably derived from JNK2. In fact, JNK2 represents most JNK activity in $T_H1$ effector cells (*14*).

To investigate the role or roles of JNK1 in $T_H$ cell activation and IL-2 production, we stimulated T cells with concanavalin A (Con A), anti-CD3, or anti-CD3 plus anti-CD28 (*12, 13*). Relative to wild-type cells, *Jnk1*$^{-/-}$ spleen cells produced the same amount of IL-2 (Fig. 2A) and CD4 T cells produced the same amount of IL-2 mRNA (*10*) 24 hours after stimulation, despite the lack of JNK activation (Fig. 1C), similar to *Jnk2*- and c-*Jun*-deficient T cells (*14, 15*). Although JNK may therefore not be required for IL-2 expression, it is also possible that JNK1 and JNK2 are redundant for IL-2 regulation. Despite normal IL-2 production, *Jnk1*$^{-/-}$ splenocytes and CD4 T cells (*10*) displayed enhanced proliferation (*12, 13*) (Fig. 2B). In addition, *Jnk1*-deficient $T_H$ cells had a

C. Dong, D. D. Yang, R. A. Flavell, Section of Immunobiology, Howard Hughes Medical Institute, Yale University School of Medicine, New Haven, CT 06520, USA. M. Wysk, A. J. Whitmarsh, R. J. Davis, Howard Hughes Medical Institute, Program in Molecular Medicine, University of Massachusetts Medical School, Worcester, MA 01605, USA.

*These authors contributed equally to this report.
†Present address: Lilly Research Laboratory, Eli Lilly and Co., Indianapolis, IN 46285, USA.
‡To whom correspondence should be addressed. E-mail: richard.flavell@qm.yale.edu